High-Spin Cation Radicals of Methylenephosphoranes

Martijn M. Wienk and René A. J. Janssen*

Contribution from the Laboratory of Organic Chemistry, Eindhoven University of Technology, P.O. Box 513, 5600 MB Eindhoven, The Netherlands

Received December 4, 1996[⊗]

Abstract: Novel di(cation radical)s and tri(cation radical)s are prepared by oxidation of the corresponding 1,3-phenylenebis[[(4-*tert*-butylphenyl)methylene]triphenylphosphorane] and 1,3,5-benzenetriyltris[[(4-*tert*-butylphenyl)-methylene]triphenylphosphorane] precursors. The oligo(cation radical)s are investigated in frozen solutions using ESR spectroscopy. The di(cation radical) has a triplet state as evidenced from a $\Delta M_s = \pm 2$ ESR transition exhibiting hyperfine coupling to two identical phosphorus nuclei and is characterized by zero-field splitting parameters $D =$ 350 MHz and $E = 0$ MHz. The corresponding tri(cation radical) possesses a quartet state with $D = 262$ MHz and $E = 0$ MHz and exhibits a $\Delta M_s = \pm 3$ transition. Temperature dependent studies (4−100 K) reveal that the ESR intensities follow Curie's law, consistent with high-spin ground states. The stability of these oligo(cation radical)s is assessed via cyclic voltammetry at room temperature in THF solution.

Introduction

High-spin molecules in which organic radicals are coupled via ferromagnetic coupling units attract considerable attention as potential building blocks for future organic ferromagnetic materials.[1−3] This interest is motivated by the fact that intramolecular coupling of unpaired electron spins is usually associated with much stronger exchange interactions than the spin alignment that can be obtained via intermolecular interactions.

In designing novel high-spin molecules, a variety of intramolecular ferromagnetic coupling units has been investigated. Several studies have shown that 1,3-connected and 1,3,5-connected benzenes act as strong and versatile ferromagnetic couplers in one and two dimensions, respectively. The *meta* substitution pattern of these units provides a non-Kékule resonance structure in which the topological symmetry and in-phase periodicity of spin polarization favor intramolecular ferromagnetic coupling of the electron spins. Using 1,3-phenylene and 1,3,5-benzenetriyl, high-spin ground state molecules have been obtained up to $S = 9$ for a nonacarbene and $S = 5$ for a deca(triarylmethyl radical).[4,5]

An important aspect of high-spin molecules is the nature of the radical center, since it determines the chemical stability and spin density at the coupling unit. For effective spin alignment, the spin density at the coupling unit must be high. In contrast, however, chemical stability usually increases with the extension of the delocalization of the unpaired electron. This inherent dichotomy has resulted in an extensive search for novel organic radicals that can be incorporated in high-spin systems. As a result various oligoradicals have been described, often containing carbon and nitrogen centered electron spins.[1−3] Although the dihedral angle between the spin-carrying unit and the ferromagnetic coupling unit is likewise important for effective coupling, 1,3-phenylene is known to be a fairly robust ferromagnetic coupling unit, even for significantly twisted geometries.[6,7]

Compared to the well-known triarylmethyl radicals, substituted diphenylmethylene ($Ph_2\dot{C}X$) radicals may provide a higher spin density at the methylene carbon atom directly linked to the 1,3-phenylene ring, which may be beneficial for a stronger exchange interaction. As an example, ketyl radicals ($Ph_2\dot{C}O^-$), which are isoelectronic with nitroxide radicals ($R_2\dot{N}O$), have recently been considered for the preparation of high-spin molecules.[8] While appealing for their stability, ketyl radicals and nitroxide radicals exhibit an appreciable delocalization of the spin density onto the oxygen nucleus, which is estimated to be on the order of 50% for nitroxide radicals.[9] Diphenylmethylenephosphorane cation radicals ($Ph_2\dot{C}PPh_3^+$) can be expected to give a higher spin density at the methylene carbon atom, because almost no direct delocalization of electron spin occurs onto the phosphorus nucleus.[10,11]

Here we describe the formation and characterization using ESR spectroscopy of two novel high-spin molecules (**1a**$^{2\bullet 2+}$ and **1b**$^{3\bullet 3+}$, Scheme 1) containing two and three methylenephosphorane cation radicals as spin centers, linked via central 1,3-phenylene and 1,3,5-benzenetriyl coupling units, respectively. The cation radicals are generated in situ via electrochemical or chemical oxidation reactions. Recently, similar procedures have been employed to generate high-spin phenylenediamine and 1,3,5-benzenetriyltriamine oligo(cation radicals).[12,13]

[⊗] Abstract published in *Advance ACS Abstracts,* May 15, 1997.

(1) Iwamura, H. *Adv. Phys. Org. Chem.* **1990**, *26*, 179.
(2) Rajca, A. *Chem. Rev.* **1994**, *94* 871.
(3) Miller, J. S.; Epstein, A. J. *Angew. Chem., Int. Ed. Engl.* **1994**, *33*, 385.
(4) (a) Nakamura, N.; Inoue, K.; Iwamura, H. *Angew. Chem., Int. Ed. Engl.* **1993**, *32*, 872. (b) Matsuda, K.; Nakamura, N.; Inoue, K.; Koga, N.; Iwamura, H. *Bull. Chem. Soc. Jpn.* **1996**, *69*, 1483.
(5) Racja, A.; Utamapanya, S.; Thayumanavan, S. *J. Am. Chem. Soc.* **1992**, *114*, 1884.
(6) Veciana, J.; Rovira, C.; Ventosa, N.; Crespo, N. I.; Palacio, F. *J. Am. Chem. Soc.* **1993**, *115*, 57.
(7) Silverman, S. K.; Dougherty, D. A. *J. Phys. Chem.* **1993**, *97*, 13273.
(8) (a) Baumgarten, M. *Mol. Cryst. Liq. Cryst.* **1995**, *272*, 109. (b) Jang, S.-H.; Mitchell, C.; Jackson, J. E.; Kahr, B. *Mol. Cryst. Liq. Cryst.* **1995**, *272*, 147.
(9) Forrester, A. R.; Hay, J. M.; Thomson, R. H. *Organic Chemistry of Stable Free Radicals*; Academic Press: London, 1968.
(10) (a) Lucken, E. A. C.; Mazeline, C. *J. Chem. Soc. A.* **1966**, 1074. (b) Lucken, E. A. C.; Mazeline, C. *J. Chem. Soc. A.* **1967**, 439.
(11) (a) Begum, A.; Lyons, A. R.; Symons, M. C. R. *J. Chem. Soc. A*, **1971**, 2388. (b) Lyons, A. R.; Neilson, G. W.; Symons, M. C. R. *J. Chem. Soc., Faraday Trans. 2* **1992**, *68*, 807.
(12) (a) Stickley, K. R.; Blackstock, S. C. *J. Am. Chem. Soc.* **1994**, *116*, 11576. (b) Stickley, K. R.; Selby, T. D.; Blackstock, S. C. *J. Org. Chem.* **1997**, *62*, 448.
(13) (a) Wienk, M. M.; Janssen, R. A. J. *Chem. Commun.* **1996**, 267. (b) Wienk, M. M.; Janssen, R. A. J. *J. Am. Chem. Soc.* **1996**, *118*, 10626. (c) Wienk, M. M.; Janssen, R. A. J. *J. Am. Chem. Soc.* **1997**, *119*, in press.

S0002-7863(96)04185-6 CCC: $14.00

Scheme 1[a]

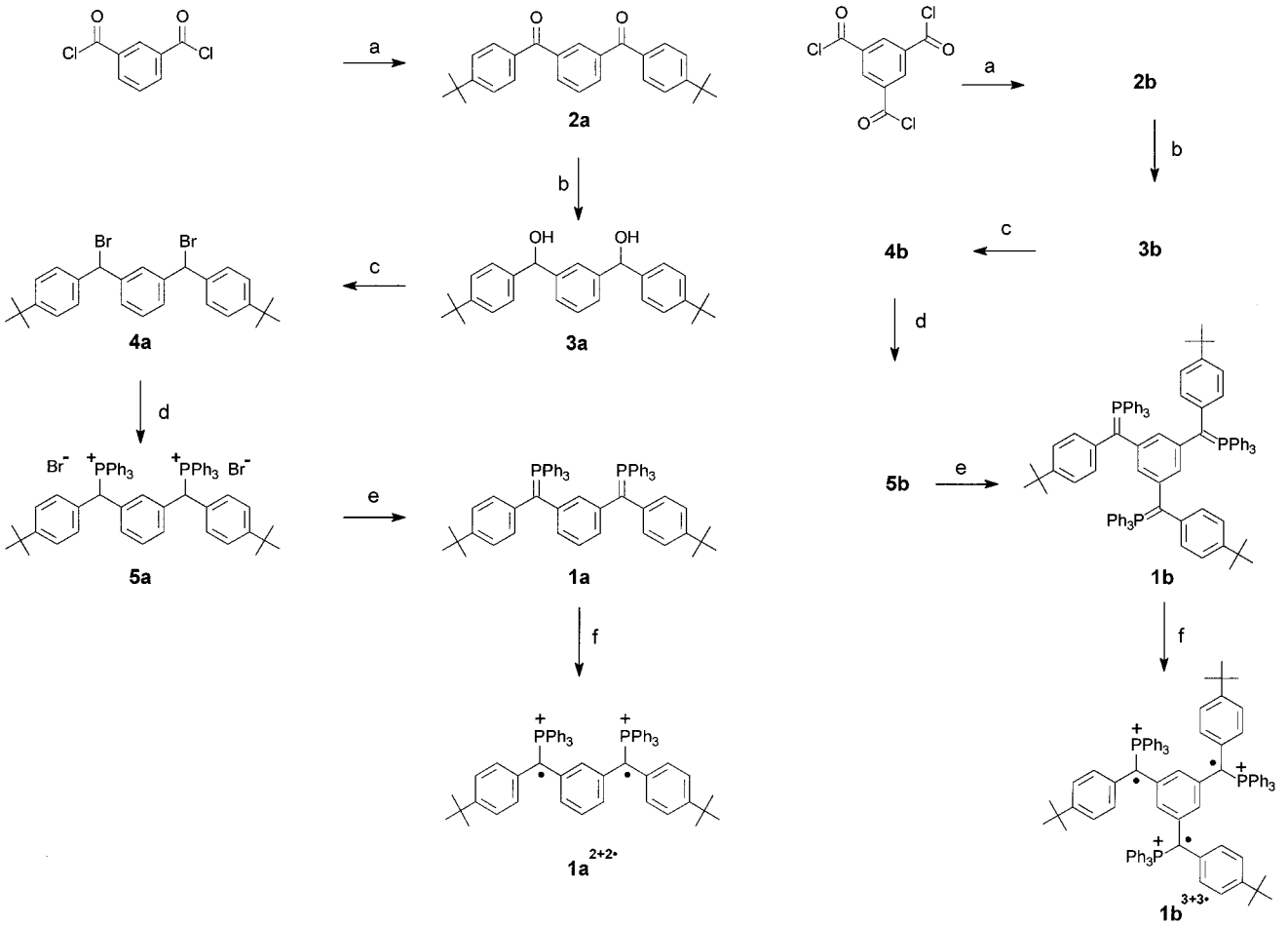

[a] (a) *tert*-butylbenzene, $AlCl_3$, CH_2Cl_2. (b) $LiAlH_4$, THF. (c) PBr_3, toluene. (d) triphenylphosphine, toluene. (e) $NaNH_2$, THF. (f) $AgBF_4$, THF.

Scheme 2

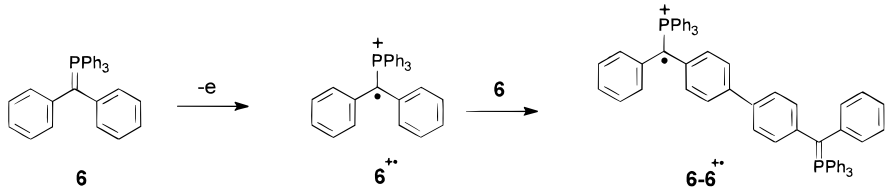

Results and Discussion

Synthesis. The synthesis of **1a** and **1b** is outlined in Scheme 1. Isophthaloyl chloride or 1,3,5-benzenetricarbonyl trichloride are reacted with *tert*-butylbenzene in a Friedel−Crafts acylation to afford 1,3-phenylene diketone (**2a**) and 1,3,5-benzenetriyl triketone (**2b**), respectively. Reduction to the corresponding diol (**3a**) and triol (**3b**) is accomplished with lithium aluminum hydride in THF, and subsequent conversion to the corresponding bromides **4a** and **4b** is carried out using phosphorus tribromide in toluene. Reaction of **4a** and **4b** with triphenylphosphine provides the bis(phosphonium bromide) **5a** and tris(phosphonium bromide) **5b**. Deprotonation of these phosphonium salts with potassium methoxide or sodium amide in THF affords the methylenephosphoranes **1a** and **1b**. These precursors are stable at −20 °C but slowly decompose at room temperature.

Cyclic Voltammetry. Cyclic voltammetry in THF solution containing 0.1 M tetrabutylammonium hexafluorophosphate (TBAH) was used to assess the stability of the different redox states of the methylenephosphoranes. The cyclic voltammogram of the parent (diphenylmethylene)triphenylphosphorane (**6,** Scheme 2) displays a quasi-reversible one-electron oxidation at 0.18 V vs SCE which is associated with the formation of a diphenylmethylenephosphorane cation radical (Figure 1). This cation radical has a limited stability, and in a second scan an additional oxidation wave is observed at −0.08 V vs SCE. This secondary product is identified using ESR (*vide infra*) as 4,4′-biphenylenebis(methylenetriphenylphosphorane) formed by coupling of the cation radical with a second molecule of **6** via the *para* positions (Scheme 2).

Cyclic voltammetry of **1a** at ambient temperature reveals two quasi-reversible one-electron oxidation waves at −0.14 and 0.23 V vs SCE (Figure 1). The quasi-reversible wave indicates that the doubly oxidized state of bis(methylenephosphorane) **1a** is moderately stable at room temperature. In this case, however, coupling reactions as observed for **6** are effectively suppressed by the *p-tert*-butyl substituents on terminal phenyl rings. In a similar experiment, one-electron oxidations of the tris(methylenephosphorane) **1b** occurred at −0.29, −0.01, and 0.27 V vs SCE (Figure 1).

The electrochemical experiments demonstrate that the first oxidation potential decreases by nearly 0.5 V when the number of methylenephosphoranes linked to the central benzene unit

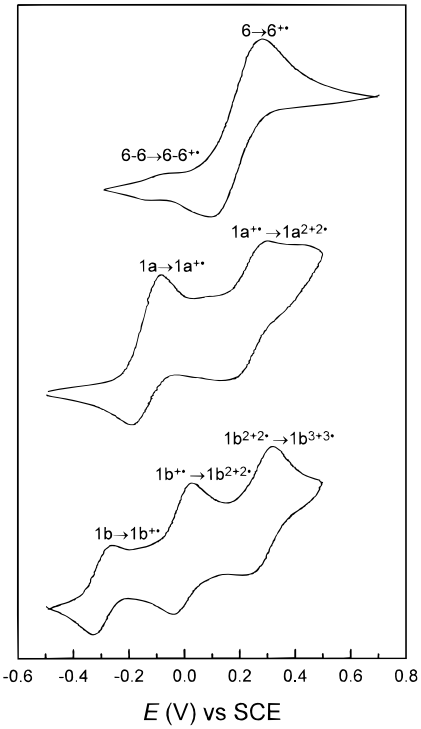

Figure 1. Cyclic voltammograms of methylenephosphoranes **6**, **1a**, and **1b** recorded in THF/TBAH (0.1 M) at 295 K, scan rate 100 mV/s, potential vs SCE calibrated against Fc/Fc^+ (0.47 V).

increases from one to three. Clearly, this decrease results from the increasing repulsive Coulombic interaction of the negative charges at the methylene carbon atoms. The effect of conjugation on the oxidation potential is likely to be small as a result of the nonresonant *meta* substitution pattern at the central ring. The final oxidation step for **6**, **1a**, and **1b** occurs at almost the same potential (0.18−0.27 V vs SCE). Similar effects have been described for perchlorotriarylmethyl anions.[6]

ESR Spectroscopy. Chemical oxidation of **6** at room temperature in THF using iodine or $AgBF_4$ produces the cation radical $\mathbf{6}^{\bullet+}$ which exhibits a well-resolved ESR spectrum due to hyperfine coupling with a phosphorus nucleus (A(P) = 74.5 MHz) and the protons of the diphenylmethylene moiety (A(*o*-H) = 7.60 MHz, A(*m*-H) = 3.28 MHz, and A(*p*-H) = 8.32 MHz) (Figure 2).[14] Under these conditions the cation radical is moderately stable. When prepared via in situ electrochemical oxidation, the ESR spectrum initially indicates the formation of $\mathbf{6}^{\bullet+}$, which under these conditions, however, rapidly couples oxidatively with a second molecule of **6** at the *para* positions to the adduct cation radical $\mathbf{6}-\mathbf{6}^{\bullet+}$. The ESR spectrum of $\mathbf{6}-\mathbf{6}^{\bullet+}$ (Figure 2) is a triplet of pentuplets resulting from hyperfine coupling with two identical ^{31}P nuclei (A(P) = 32.82 MHz) and four identical ^{1}H nuclei (A(H) = 4.96 MHz, at 3-, 3′-, 5-, and 5′-positions), identical to the ESR spectrum obtained via oxidation of 4,4′-biphenylenebis[phenylmethylenetriphenylphosphorane] (**6**−**6**).[15] When electrochemical oxidation is carried out at 240 K, the coupling reaction is suppressed.

To prevent side reactions, chemical oxidation of the bis- and trismethylenephosphoranes **1a** and **1b** was carried out at 195 K. At that temperature chemical oxidation of **1a** with $AgBF_4$ in THF initially produces the corresponding mono(cation radical) $\mathbf{1a}^{\bullet+}$, which is characterized by a partially resolved ESR spectrum. Hyperfine interactions with one ^{31}P nucleus (A(P) = 72.5 MHz) and three different sets of two equivalent ^{1}H nuclei (A(H) = 11.5, 3.75, and 2.75 MHz) indicate appreciable spin delocalization over both the terminal and central benzene rings. Further oxidation of $\mathbf{1a}^{\bullet+}$ produces $\mathbf{1a}^{2\bullet2+}$. The anisotropic ESR spectrum recorded in frozen THF at 120 K reveals a superposition of the spectra of the mono(cation radical) and the triplet di(cation radical) (Figure 3). The two strong central transitions are attributed to the mono(cation radical) $\mathbf{1a}^{\bullet+}$, possessing an essentially isotropic ^{31}P hyperfine coupling. The broad lines in the lateral regions of the spectrum are the $\Delta M_s = \pm1$ transitions of the di(cation radical) $\mathbf{1a}^{2\bullet2+}$, exhibiting a zero-field splitting characteristic of a triplet state. Weak shoulders on the *xy* components of the ESR spectrum of $\mathbf{1a}^{2\bullet2+}$ are tentatively attributed to partially resolved ^{31}P hyperfine coupling. Further evidence for the formation of di(cation radical) $\mathbf{1a}^{2\bullet2+}$ in a triplet state is obtained from the ESR spectrum recorded in the $g = 4$ region, where the formally forbidden $\Delta M_s = \pm2$ transition of $\mathbf{1a}^{2\bullet2+}$ is observed (Figure 3). The $\Delta M_s = \pm2$ ESR spectrum exhibits a well-resolved 1:2:1 three-line pattern resulting from hyperfine interaction of the $S = 1$ spin with two

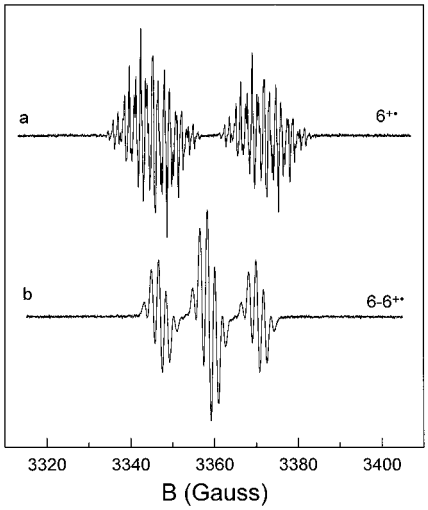

Figure 2. ESR spectra of (a) cation radical $\mathbf{6}^{\bullet+}$ obtained via iodine oxidation of **6** in THF. (b) The adduct cation radical $\mathbf{6}-\mathbf{6}^{\bullet+}$, prepared via electrochemical oxidation of **6** in THF/TBAH (0.1 M). Hyperfine parameters are described in the text.

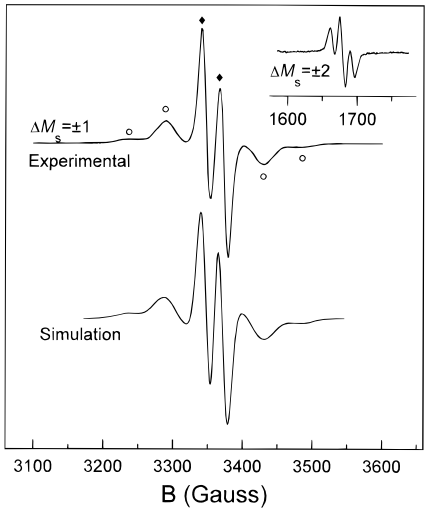

Figure 3. $\Delta M_s = \pm1$ ESR spectrum of **1a** recorded in THF at 120 K after oxidation with $AgBF_4$, showing the transitions assigned to $\mathbf{1a}^{\bullet+}$ (◆) and $\mathbf{1a}^{2\bullet2+}$ (○). The simulation is a 2:5 superposition of the spectra of mono(cation radical) $\mathbf{1a}^{\bullet+}$ and a di(cation radical) $\mathbf{1a}^{2\bullet2+}$ calculated using the zero-field and hyperfine coupling parameters described in the text. The inset shows the $\Delta M_s = \pm2$ ESR spectrum of $\mathbf{1a}^{2\bullet2+}$.

(14) Buck, H. M.; Huizer, A. H.; Oldenburg, S. J.; Schipper, P. *Recl. Trav. Chim.* **1970**, *89*, 1085.

(15) Kooistra, C.; van Dijk, J. M. F.; van Lier, P. M.; Buck, H. M. *Recl. Trav. Chim.* **1973**, *92*, 961.

equivalent ^{31}P nuclei, which exhibit half the hyperfine coupling constant observed for mono(cation radical) **1a**$^{\bullet+}$. The identical hyperfine coupling to two ^{31}P nuclei directly relates the spectrum to the proposed structure of **1a**$^{2\bullet2+}$. Apart from the intensity, the ESR spectrum does not change in the temperature range of 4 to 130 K.

The ESR spectrum of mono(cation radical) **1a**$^{\bullet+}$ can be simulated assuming an isotropic ^{31}P hyperfine coupling constant of A(P) = 65 MHz and a Gaussian line width of 48 MHz.[16] The hyperfine coupling constant of **1a**$^{\bullet+}$ was used as starting point to obtain a spectral simulation for **1a**$^{2\bullet2+}$. We found that the remaining transitions in the ESR spectrum attributed to **1a**$^{2\bullet2+}$ are reproduced satisfactorily by taking D = 350 MHz and E = 0 MHz for the zero-field splitting parameters, an isotropic hyperfine constant of A(P) = 32.5 MHz (i.e., half the coupling constant of **1a**$^{\bullet+}$), and using a Gaussian line width of 85 MHz (Figure 3).[17] The increased line width of **1a**$^{2\bullet2+}$ as compared to **1a**$^{\bullet+}$ explains the loss of hyperfine structure in the $\Delta M_s = \pm1$ triplet spectrum. Adding the simulated spectra of **1a**$^{\bullet+}$ and **1a**$^{2\bullet2+}$ in a 2:5 ratio provides a good agreement with the experimental spectrum (Figure 3) and demonstrates the fairly efficient production of di(cation radical)s.

The zero-field splittings and hyperfine couplings obtained from the spectral simulation can be used to assess the electronic structure of **1a**$^{\bullet+}$ and **1a**$^{2\bullet2+}$ in some detail. The isotropic hyperfine coupling A(P) = 65 MHz of **1a**$^{\bullet+}$ suggests that the spin density at the methylene carbon is about 57%, when compared to A(P) = 114 MHz of the methylenetriphenylphosphorane cation radical ($Ph_3PCH_2^{\bullet+}$), for which unit spin density on carbon can be assumed.[10b] The zero-field splitting of D = 350 MHz for **1a**$^{2\bullet2+}$ is significantly larger than the value of 237 MHz reported for Schlenk's biradical. This indicates an increased spin density on the methylene carbon for a diphenylmethylenephosphorane cation radical as compared to a triarylmethyl radical.[18] The D value of 350 MHz for **1a**$^{2\bullet2+}$ corresponds within the point-dipole approximation to a distance between the radical centers of about 6.1 Å. Standard bond lengths suggest a distance of only 4.85 Å between the two methylene carbon nuclei. The difference can be interpreted as an indication for some localization of spin density in the terminal 4-*tert*-butylphenyl rings which may result from a twisting of the methylene carbons out of the plane of conjugation with the central 1,3-phenylene unit as consequence of steric hindrance.

Variable temperature experiments in the range from T = 3.8 to 100 K on the $\Delta M_s = \pm1$ and $\Delta M_s = \pm2$ ESR transitions of **1a**$^{2\bullet2+}$ demonstrate that the signal intensity follows Curie's law ($I = C/T$), indicating that the population of the triplet state is independent of temperature (Figure 4). Hence, the triplet state is separated from the corresponding singlet state by either a very large or a very small energy gap. Although it is not possible to resolve this ambiguity using ESR, it can be concluded that in either case the triplet state corresponds to a low-energy state.[19]

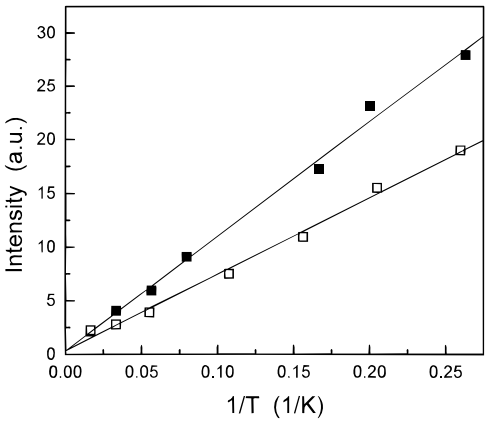

Figure 4. Temperature dependence of ESR signal intensity of the $\Delta M_s = \pm1$ (■) and $\Delta M_s = \pm2$ (□) transitions of di(cation radical) **1a**$^{2\bullet2+}$. Solid lines are least-square fits to Curie's law.

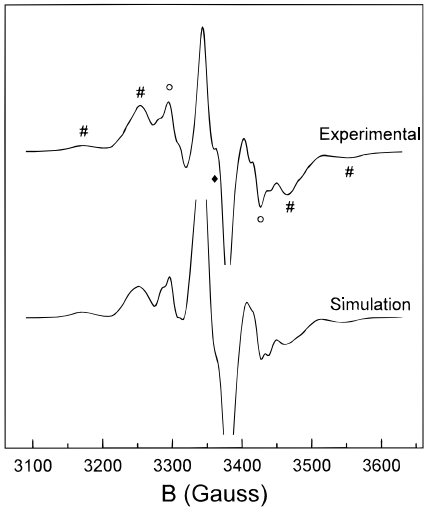

Figure 5. $\Delta M_s = \pm1$ ESR spectrum of **1b** recorded in THF at 120 K after oxidation with $AgBF_4$, showing the transitions assigned to **1b**$^{\bullet+}$-(◆), **1b**$^{2\bullet2+}$(○), and **1b**$^{3\bullet3+}$(#). The simulation is a 1:6:14 superposition of the spectra of mono(cation radical) **1b**$^{\bullet+}$, di(cation radical) **1b**$^{2\bullet2+}$, and tri(cation radical) **1b**$^{3\bullet3+}$ calculated using the zero-field and hyperfine coupling parameters described in the text.

The ESR spectrum of **1b** recorded at 150 K after oxidation with $AgBF_4$ in THF at 195 K reveals the presence of the corresponding mono(cation radical)**,** di(cation radical)**,** and tri-(cation radical) (Figure 5). In the central region of the ESR spectrum, the strong partially-resolved ^{31}P doublet of **1b**$^{\bullet+}$ is observed, accompanied on each side by the transitions of triplet-state **1b**$^{2\bullet2+}$ showing some poorly resolved hyperfine structure. The broad lines in the outer parts are attributed to the $\Delta M_s = \pm1$ transitions of **1b**$^{3\bullet3+}$ in a quartet state. The appearance of the ESR spectrum does not change between 4 and 130 K, apart from intensity. The presence of high-spin states can further be inferred from the ESR spectra at lower fields. In the g = 4 region (Figure 6) the 1:2:1 three-line pattern of the $\Delta M_s = \pm2$ transition of **1b**$^{2\bullet2+}$ is observed, resulting from a triplet state with a hyperfine coupling to two identical ^{31}P nuclei with a coupling constant of about 33 MHz. In the outer regions of the half-field spectrum a weak pattern can be discerned which is attributed to the $\Delta M_s = \pm2$ signal of **1b**$^{3\bullet3+}$ in a quartet state. The $\Delta M_s = \pm2$ spectrum of a quartet state is expected to exhibit

(16) The apparent decrease of A(P) in the spectrum recorded in frozen THF matrix at 120 K as compared to the isotropic coupling of 72.5 MHz in THF solution at 195 K, is readily explained by a small anisotropy of the ESR spectrum, which is dominated by the perpendicular couplings. In fact, an equally adequate simulation for **1a**$^{\bullet+}$ can be obtained using an axially symmetric hyperfine tensor with principal values A(P) = 89.5, 64, and 64 MHz, consistent with an isotropic coupling of A(P) = 72.5 MHz. However, since this anisotropy is not resolved in the spectrum, we favor a description using only one parameter.

(17) Simulations show that the weak shoulders in the experimental ESR spectrum of **1a**$^{2\bullet2+}$ can be due to unresolved hyperfine coupling, an $E \neq 0$ value, or a combination thereof. The limited resolution does not allow discrimination between these possibilities.

(18) Kothe, G.; Denkel, K.-H.; Sümmermann, W. *Angew. Chem.* **1970**, *82,* 935.

(19) Berson, J. A. In *The Chemistry of Quinoid Compounds*; Patai, S., Rappaport, Z. Eds.; Wiley: 1988; Vol II, Chapter 10.

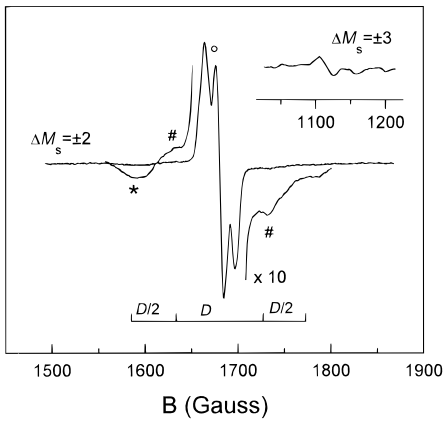

Figure 6. $\Delta M_s = \pm 2$ ESR spectrum of di(cation radical) $\mathbf{1b}^{2\bullet 2+}$ (○) and tri(cation radical) $\mathbf{1b}^{3\bullet 3+}$ (#). The signal marked with an asterisk is a background signal. The inset shows the $\Delta M_s = \pm 3$ ESR spectrum of $\mathbf{1b}^{3\bullet 3+}$.

four lines with a spacing of $D/2$, D, and $D/2$ respectively.[20,21] Experimentally, the two inner lines appear as clear shoulders on the $\Delta M_s = \pm 2$ transition of $\mathbf{1b}^{2\bullet 2+}$, while the outer two lines could not be identified with certainty. The spectral intensity of the $\Delta M_s = \pm 2$ transition of $\mathbf{1b}^{3\bullet 3+}$ is considerably reduced compared to the $\Delta M_s = \pm 2$ transition of $\mathbf{1b}^{2\bullet 2+}$ as a result of the increased spectral width. Direct spectral evidence of a quartet state for $\mathbf{1b}^{3\bullet 3+}$ is obtained in the $g = 6$ region, where the $\Delta M_s = \pm 3$ transition is observed. This leaves no doubt on the formation of a quartet state. In literature only few organic polyradicals have been reported that exhibit a $\Delta M_s = \pm 3$ transition in the ESR spectrum.[8a,21−23]

The spectral simulation of the $g = 2$ region of the mixture of the three oxidation states $\mathbf{1b}^{\bullet +}$, $\mathbf{1b}^{2\bullet 2+}$, and $\mathbf{1b}^{3\bullet 3+}$ is shown in Figure 5. For this simulation the hyperfine and zero-field parameters of $\mathbf{1b}^{\bullet +}$ ($S = 1/2$, A(P) = 65 MHz, Gaussian line width of 45 MHz) and $\mathbf{1b}^{2\bullet 2+}$ ($S = 1$, $D = 350$, $E = 0$, A(P) = 32.5 MHz, Gaussian line width of 32 MHz) are identical to those of $\mathbf{1a}^{\bullet +}$ and $\mathbf{1a}^{2\bullet 2+}$. In contrast to $\mathbf{1a}^{2\bullet 2+}$, the A(P) hyperfine coupling of $\mathbf{1b}^{2\bullet 2+}$ is partially resolved due to a reduced line width of the triplet spectrum. For $\mathbf{1b}^{3\bullet 3+}$ we found that the experimental spectrum can be simulated by taking $S = 3/2$, $D = 262$, $E = 0$ MHz and a Gaussian line width of 98 MHz (no ^{31}P hyperfine coupling was used in this case). By adding the spectra of $\mathbf{1b}^{\bullet +}$, $\mathbf{1b}^{2\bullet 2+}$, and $\mathbf{1b}^{3\bullet 3+}$ in a 1:6:14 ratio, an acceptable correspondence was obtained with the experimental spectrum. Although the point-dipole approximation for a triradical is not straightforward, the decreased zero-field splitting for $\mathbf{1b}^{3\bullet 3+}$ ($D = 262$ MHz) as compared to $\mathbf{1a}^{2\bullet 2+}$ and $\mathbf{1b}^{2\bullet 2+}$ ($D = 350$ MHz) suggests a rise in average distance between the unpaired electrons from 6.1 to 6.7 Å.

The signals at $g = 4$ and $g = 6$ of $\mathbf{1b}^{3\bullet 3+}$ were too weak to be measured accurately at temperatures above 4 K, but the $\Delta M_s = \pm 1$ transitions follow Curie's law, when changing the temperature in the range from $T = 3.8$ to 100 K (Figure 7). We conclude that the quartet state of $\mathbf{1b}^{3\bullet 3+}$ is the ground state, although an exact degeneracy with the corresponding doublet state cannot be excluded from this experiment.[19]

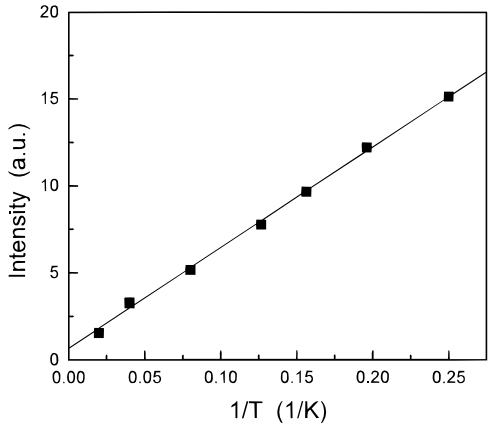

Figure 7. Temperature dependence of ESR signal intensity of the $\Delta M_s = \pm 1$ (■) transition of tri(cation radical) $\mathbf{1b}^{3\bullet 3+}$. Solid line is a least-square fit to Curie's law.

Conclusion

Novel oligo(cation radical)s $\mathbf{1a}^{2\bullet 2+}$ and $\mathbf{1b}^{3\bullet 3+}$ have been prepared by chemical oxidation of the corresponding oligo(methylenephosphoranes). These oligo(cation radical)s have been fully characterized using ESR spectroscopy and are found to possess a triplet and quartet ground state, respectively, as a consequence of the *meta* substitution pattern at the central benzene ring.

Experimental Section

General Methods. Commercial grade reagents were used without further purification. Solvents were purified, dried, and degassed following standard procedures. NMR spectra were recorded on a Bruker AM-400 spectrometer, and chemical shifts are relative to TMS for ^{1}H and ^{13}C-NMR spectra and relative to aqueous 85% H_3PO_4 solution (external standard) for ^{31}P NMR spectra. Cyclic voltammograms were recorded with 0.1 M tetrabutylammonium hexafluorophosphate as supporting electrolyte using a Potentioscan Wenking POS73 potentiostat. The working electrode was a platinum disc (0.2 cm^2), the counter electrode was a platinum plate (0.5 cm^2), and a saturated calomel electrode was used as reference electrode, calibrated against a Fc/Fc$^+$ couple. ESR spectra were recorded on a Bruker ER 200D spectrometer, operating with an X-band standard or TMH cavity, interfaced to a Bruker Aspect 3000 data system. Temperature was controlled by a Bruker ER4111 variable-temperature unit between 100 and 300 K or by an Oxford 3120 temperature controller combined with an ESR900 continuous flow cryostat in the range 4−100 K. Saturation of the ESR signal during variable temperature experiments was avoided by using low microwave powers, *i.e.*, 200 nW for the $\Delta M_s = \pm 1$ transition and 1 mW for the $\Delta M_s = \pm 2$ transition, which is well within the range where signal intensity is proportional to the square root of the microwave power at 4 K.

1,3-Phenylenebis[(4-*tert*-butylphenyl)methanone] 2a. Isophthaloyl chloride (10.15 g, 0.05 mol) in CH_2Cl_2 (20 mL) was added slowly to a suspension of $AlCl_3$ (16.0 g, 0.12 mol) in CH_2Cl_2 (50 mL) with stirring and cooling in an ice bath. Then *tert*-butylbenzene (16.1 g, 0.12 mol) was added keeping the temperature at 20 °C. After stirring for 18 h at room temperature the mixture was poured onto ice. The organic phase was separated, and the aqueous phase was extracted with CH_2Cl_2. The combined organic fractions were washed with dilute NaOH solution and water and dried over $MgSO_4$. Evaporation of the solvent and recrystallization from ethanol afforded pure **2** (14.6 g, 74%) as a white crystalline material: mp 153 °C; ^{1}H NMR ($CDCl_3$) δ 1.36 (18H, s, CH_3), 7.51 (4H, d, $J = 8.6$ Hz, H-2′), 7.62 (1H, t, $J = 7.7$ Hz, H-5), 7.78 (4H, d, $J = 8.6$ Hz, H-3′), 8.02 (2H, dd, $J = 7.7$ Hz and 1.8 Hz, H-4), 8.17 (1H, t, $J = 1.8$ Hz, H-2); ^{13}C NMR ($CDCl_3$): δ 31.10 (CH_3), 35.16 (CCH_3), 125.44 (C-3′), 128.41 (C-5), 130.17 (C-2′), 131.13 (C-2), 133.21 (C-4), 134.26 (C-1), 138.01 (C-1′), 156.67 (C-4′), 195.63 (CO).

(20) Brickmann, J.; Kothe, G. *J. Chem. Phys.* **1973**, *59*, 2807.
(21) (a) Rajca, A.; Utamapanya, S. *J. Am. Chem. Soc.* **1993**, *115*, 2396. (b) Rajca, A.; Rajca, S.; Desai, S. R. *J. Am. Chem. Soc.* **1995**, *117*, 806.
(22) Weissman, S. I.; Kothe, G. *J. Am. Chem. Soc.* **1975**, *97*, 2537.
(23) Müller, U.; Baumgarten, M. *J. Am. Chem. Soc.* **1995**, *117*, 5840.
(24) Different signals arise from diastereoisomeric *RS* and *RR* + *SS* isomers.
(25) One signal arises from *RRR* + *SSS* isomers, the other two from the *RRS* and *SSR* isomers which contain two inequivalent phosphorus nuclei.

1,3,5-Benzenetriyltris[(4-*tert*-butylphenyl)methanone] 2b. From 1,3,5-benzenetricarbonyl trichloride (2.65 g, 10 mmol) using same procedure as for **2a**. Yield (3.52 g, 63%) as white crystals: mp 181 °C; ^{1}H NMR ($CDCl_3$) δ 1.36 (27H, s, CH_3), 7.53 (6H, d, J = 8.4 Hz, H-2′), 7.81 (6H, d, J = 8.4 Hz, H-3′), 8.39 (3H, s, H-2); ^{13}C NMR ($CDCl_3$): δ 31.03 (CH_3), 35.14 (CCH_3), 125.56 (C-3′), 130.16 (C-2′), 133.80 (C-1 + C-2), 138.36 (C-1′), 157.03 (C-4′), 194.67 (CO).

α,α′-Bis(4-*tert*-butylphenyl)-1,3-benzenedimethanol 3a. Compound **2a** (9.96 g, 25 mmol) in THF (50 mL) was added slowly to a suspension of $LiAlH_4$ (1.9 g, 50 mmol) in THF (50 mL) with stirring and cooling in an ice bath. After the addition was complete, the ice bath was removed, and the mixture was stirred at room temperature for 30 min. Then water was added carefully to quench the excess of $LiAlH_4$. The mixture was concentrated and extracted with diethyl ether. The collected organic fractions were washed with water and dried with $MgSO_4$, and the solvent was evaporated affording pure **3a** (9.73 g, 97%) as a white solid: ^{1}H NMR ($CDCl_3$) δ 1.29 (18H, s, CH_3), 2.15 (2H, b s, OH), 5.77 (2H, 2 s, C*H*OH), 7.24−7.34 (11H, m, H-4, H-5, H-2′, H-3′), 7.47, 7.49 (1H, 2 s, H-2); ^{13}C NMR ($CDCl_3$): δ 31.32 (CH_3), 34.48 (CCH_3), 76.00 (COH), 124.59, 124.62 (C-2), 125.39 (C-3′), 125.55, 125.65 (C-4), 126.30, 126.35 (C-2′), 128.53 (C-5), 140.76 (C-1′), 144.02, 144.08 (C-1), 150.51 (C-4′).

α,α′,α″-Tris(4-*tert*-butylphenyl)-1,3,5-benzenetrimethanol 3b was obtained from **2b** (2.24 g, 4 mmol) using the same procedure as for **3a**. Yield (2.16 g, 96%) as a white solid: ^{1}H NMR ($CDCl_3$) δ 1.29 (27H, s, CH_3), 3.2 (3H, 2 b s, OH) 5.67 (3H, m, C*H*OH), 7.24−7.34 (15H, m, H-2, H-2′, H-3′); ^{13}C NMR ($CDCl_3$): δ 31.27 (CH_3), 34.39 (CCH_3), 75.76, 75.80 (COH), 123.83 (C-2), 125.22 (C-3′), 126.34, 126.36 (C-2′), 140.63 (C-1′), 144.21, 144.27 (C-1), 150.22 (C-4′).

1,3-Bis[bromo(4-*tert*-butylphenyl)methyl]benzene 4a. PBr_3 (5.41 g, 20 mmol) in toluene (40 mL) was added slowly to a stirred suspension of **3a** (4.02 g, 10 mmol) in toluene (20 mL) at room temperature. The solution became clear and was stirred for 1 h. The mixture was poured onto ice and extracted two times with toluene. The combined organic layers were washed with water and dried over $MgSO_4$, and the solvent was evaporated affording pure **4a** (4.91 g, 93%) as a light yellow solid: ^{1}H NMR ($CDCl_3$) δ 1.30 (18H, s, CH_3), 6.25 (2H, 2 s, CHBr), 7.2−7.4 (11H, m, H-4, H-5, H-2′, H-3′), 7.62 (1H, s, H-2); ^{13}C NMR ($CDCl_3$): δ 31.23 (CH_3), 34.57 (CCH_3), 54.96 (CBr), 125.54 (C-3′), 128.09 (C-2′), 128.15 (C-4), 128.58, 128.70 (C-2, C-5), 137.74, 137.81 (C-1′), 141.27, 141.39 (C-1), 151.22 (C-4′).

1,3,5-Tris[bromo(4-*tert*-butylphenyl)methyl]benzene 4b was obtained from **3b** (1.69 g, 3 mmol) using the same procedure as described for **4a**. Yield (2.05 g, 91%) as a light brown solid: ^{1}H NMR ($CDCl_3$) δ 1.29 (27H, s, CH_3), 6.22 (3H, m, CHBr), 7.2−7.4 (15H, m, H-2′, H-3′), 7.55 (3H, m, H-2); ^{13}C NMR ($CDCl_3$): δ 31.22 (CH_3), 34.58 (CCH_3), 54.45 (CBr), 125.60 (C-3′), 129.09 (C-2′), 128.35 (C-2), 137.43, 137.53, 137.63 (C-1′), 141.46, 141.59, 141.75 (C-1), 151.35 (C-4′).

1,3-Phenylenebis{[(4-*tert*-butylphenyl)methyl]triphenylphosphonium bromide} 5a. A solution of **4a** (1.06 g, 2 mmol) and triphenylphosphine (1.31 g, 5 mmol) was heated under reflux for 24 h. After cooling, the solvent was evaporated. Column chromatography (SiO_2, $CHCl_3$/MeOH 95:5−9:1) afforded pure **5a** (0.90g, 43%) as a white solid. ^{31}P NMR ($CDCl_3$) δ 23.14, 23.18.[24] ES-MS *m/z* (M − Br^-) calcd 971.4, obsd 971.3.

1,3,5-Benzenetriyltris{[(4-*tert*-butylphenyl)methyl]triphenylphoshonium bromide} 5b was obtained from **4b** (0.75 g, 1 mmol) using the same procedure as described for **5a**. Yield (0.60 g, 41%) as a white solid: ^{31}P NMR($CDCl_3$) δ 23.34, 23.78, 24,08.[25] ES-MS *m/z* (M − Br^-) calcd 1457.5, obsd 1457.5.

1,3-Phenylenebis[[(4-*tert*-butylphenyl)methylene]triphenylphosphorane] 1a. $NaNH_2$ (4.0 mg, 0.1 mmol) was added to a suspension of **5a** (21 mg, 0.02 mmol) in THF (2 mL) at room temperature. The reaction mixture quickly turned deep red. After stirring at room temperature for 1 h, the conversion was complete as evidenced by NMR spectroscopy, using a small aliquot of the reaction mixture: ^{31}P NMR (THF) δ 6.39; ^{1}H NMR (THF) δ 6.25 (2H, d, J = 8.0 Hz, H-4), 6.31 (4H, d, J = 8.6 Hz, H-2′), 6.36 (1H, t, J = 8.0 Hz, H-5), 6.61 (4H, d, J = 8.6 Hz, H-3′), 6.73 (1H, s, H-2), 7.23−7.30 (12 H, m, H-3″), 7.33−7.39 (6H, m, H-4″), 7.41−7.48 (12H, m, H-3″).

1,3,5-Benzenetriyltris[[(4-*tert*-butylphenyl)methylene]triphenylphosphorane] 1b. From **5b** (0.75 g, 1 mmol) using the same procedure as described for **1a**: ^{31}P NMR (THF) δ 5.80; ^{1}H NMR (THF) δ 6.06 (6H, d, J = 8.3 Hz, H-2′), 6.33 (3H, s, H-2), 6.54 (6H, d, J = 8.3 Hz, H-3′), 7.21−7.26 (18 H, m, H-3″), 7.29−7.45 (27H, m, H-2″ + H-4″).

Oxidation of Bis(methylenephosphorane) 1a. A freshly prepared solution of phosphorane **1a** (0.02 mmol) in THF (2 mL) was cooled to −78 °C in a Schlenk vessel, and a solution of $AgBF_4$ (0.5 mL, 0.08 M in THF) was added slowly by syringe. After stirring at −78 °C for 30 min, the mixture was transferred as quickly as possible into a precooled ESR tube equipped with a ground-glass joint. After sealing, the sample was cooled to 77 K using liquid nitrogen.

Oxidation of tris(methylenephosphorane) 1b was performed using from freshly prepared **1b** (0.02 mmol) in THF (2 mL) and $AgBF_4$ (0.75 mL, 0.08 M in THF), following the same procedure as described for the oxidation of **1a**.

Acknowledgment. We thank Professor E. W. Meijer for valuable discussions and Philips Research for an unrestricted research grant. This work has been supported by the Netherlands Foundation for Chemical Research (SON) with financial aid from the Netherlands Organization for Scientific Research (NWO).

JA964185E